Biosensors and Bioelectronics 43 (2013) 218–225

Contents lists available at SciVerse ScienceDirect

Biosensors and Bioelectronics

journal homepage: www.elsevier.com/locate/bios

# Label-free electrochemical IgE aptasensor based on covalent attachment of aptamer onto multiwalled carbon nanotubes/ionic liquid/chitosan nanocomposite modified electrode

Somayeh Khezrian [a], Abdollah Salimi [a,b,*], Hazhir Teymourian [a], Rahman Hallaj [a]

[a] Department of Chemistry, University of Kurdistan, P. O. Box 416, Sanandaj, Iran
[b] Research Center for Nanotechnology, University of Kurdistan, P.O. Box 416, Sanandaj, Iran

ARTICLE INFO

*Article history:*
Received 14 June 2012
Received in revised form
25 November 2012
Accepted 4 December 2012
Available online 20 December 2012

*Keywords:*
Label-free aptasensor
Immunoglobulin E
Chitosan
Ionic liquid
Carbon nanotubes

ABSTRACT

A simple, sensitive and label-free aptamer-based biosensor for the detection of human immunoglobulin E (IgE) is developed using the electrochemical transduction method. A special immobilization interface consisting of multiwalled carbon nanotubes/ionic liquid/chitosan nanocomposite (MWCNTs/IL/Chit) is utilized to improve the conductivity and performance characteristics of the biosensor as well as to increase the loading amount of aptamer DNA sequence. A 5'-amino-terminated aptamer is covalently attached onto MWCNTs/IL/Chit modified glassy carbon (GC) electrode via a linker of glutaraldehyde (GA). Methylene blue (MB) is used as an electrochemical indicator which is intercalated into the aptamer through the specific interaction with its guanine bases. In the absence of IgE, MB bound to the aptamer produces a strong differential pulse voltammetric (DPV) signal. But when IgE exists, the intercalated MB releases from the aptamer, resulting an obviously decreased DPV signal. This phenomenon can be applied for human IgE detection. The peak current of MB linearly decreases with the concentration of IgE over a range of 0.5–30 nM with a detection limit of 37 pM. By using Bovine serum albumin (BSA) and lysozyme, the excellent specificity of this sensing system for the detection of IgE is also demonstrated. Finally, the proposed aptasensor is successfully used to IgE analysis in human serum sample. The obtained result is well agreed with the value obtained by the standard ELISA method. The herein described approach is expected to promote the exploitation of aptamer-based biosensors for protein assays in biochemical and biomedical studies.



## 1. Introduction

Since the pioneering studies on aptamers (Ellington and Szostak, 1990; Tuerk and Gold, 1990), substantial research efforts have been directed in order to apply the aptamers as the active sensing materials in different detection schemes (Zayats et al., 2006), led to the development of various electrical (Radi et al., 2005; Xu et al., 2005; Wu et al., 2009), microgravimetric (Pavlov et al., 2004; Yao et al., 2009) and optical aptasensors (Nutiu and Li, 2003; Ho and Leclerc, 2004; Gokulrangan et al., 2005). Aptamers are artificial nucleic acid ligands showing specific binding affinity for amino acids, drugs, proteins and other small molecules, which can be screened through the systematic evolution of ligands by exponential enrichment (SELEX) process from random RNA or DNA libraries (Tuerk and Gold, 1990; Ellington and Szostak, 1990). Compared with antibodies, aptamers possess some outstanding features, including high specificity of binding affinity, nice stabilization, easy synthesis and modification with electrochemical active markers, optical dyes, enzymes and other desired substances. Furthermore, aptamers can reversibly capture and release their target molecule. It is more facile for the aptamer to transduce the recognition events into detectable signals (Kang et al., 2008).

Among the various sensing devices developed so far, the detection methods of label-free, aptamer-based electrochemical biosensors have received an increasing amount of attention due to their inherent advantages such as simplicity, high sensitivity, low cost and high stability (Cheng et al., 2007; Feng et al., 2008; Wang et al., 2009a; Yan et al., 2011). Many of these electrochemical methods are based on electrochemical redox indicators that bind to the nucleic acids via electrostatic interactions or intercalation. Methylene blue (MB) is a widely-used redox indicator that belongs to phenothiazine family and is an aromatic cationic dye showing optically and electrochemically active properties. It has been proved that MB could intercalate the nucleic acid duplexes

* Corresponding author at: Department of Chemistry, University of Kurdistan, P.O. Box 416, Sanandaj, Iran. Tel.: +98 871 6624001; fax: +98 871 6624008.
*E-mail addresses:* absalimi@uok.ac.ir, absalimi@yahoo.com (A. Salimi).

0956-5663/$ - see front matter © 2012 Elsevier B.V. All rights reserved.
http://dx.doi.org/10.1016/j.bios.2012.12.006

(Kerman et al., 2002) and also bind to guanine bases specifically (Kara et al., 2002). This feature has been extensively used to develop DNA-based biosensors (Du et al., 2009; Liu et al., 2011).

Concerning the construction of an electrochemical biosensor, modifying the electrode surface with nanomaterials to exploit their superior properties seems to be more promising and provides more efficient electron transfer between the matrix electrode and biomolecules (Gooding et al., 2003). Among different nanomaterials, carbon nanotubes (CNTs) are considered as an important group of nanostructures with attractive electronic, chemical and mechanical properties (Rao et al., 2001; Baughman et al., 2002). The compatibility and electrochemical applications of CNTs to immobilize a variety of species on their external and internal surfaces have been reported (Chen et al., 2001; Salimi et al., 2006, 2007; Teymourian et al., 2012a, 2012b). However, it is noted that CNTs, which have a high specific surface area, tend to form irreversible agglomerates through strong π–π stacking and the van der Waals interaction (Li et al., 2008). Hence, the prevention of aggregation is a key challenge in the synthesis and processing of bulk quantity of CNTs. Ionic liquids (ILs) can meet this challenge well. CNTs can be well dispersed in ILs due to cation–π interactions and a CNTs/ILs paste can easily be prepared using ILs as the binder, where the CNTs greatly enhances the conductivity of the system (Fukushima et al., 2003; Wang et al., 2007). Through combining the benefits of ILs and CNTs for electrochemical sensing applications, a remarkable synergistic augmentation of electrochemical performance can be achieved increasing the potential application of CNTs/ILs in fabrication of electrochemical sensors and biosensors (Salimi et al., 2010; Teymourian et al., 2012a).

Immunoglobulin E (IgE) was selected in this work as the model target protein. IgE is an antibody subclass, found only in mammals (Sutton and Gould, 1993). IgE is also capable of triggering the most powerful immune reactions and its rapid detection is of great interest in dealing with patients afflicted with allergy-mediated disorders (Maehashi et al., 2007). Although some aptamer-based assays have been reported for the IgE detection utilizing distinct signal transduction mechanisms including SPR (Wang et al., 2008; Kim et al., 2009), luminescence (Jiang et al., 2004), fluorescence polarization (Gokulrangan et al., 2005), electrochemical impedance spectroscopy (Xu et al., 2005), FET (Maehashi et al., 2007), quartz crystal microbalance (Yao et al., 2009) and voltammetric-based aptasensors (Papamichael et al., 2007;.Wu et al., 2009), there is no demonstration of an analytical paradigm in this respect. Most of these methods suffer from some disadvantages, such as lack of sensitivity, high cost instrumentation, complex strategies (for example; various sandwich assays or prelabeling the aptamer) and utilizing a difficult aptamer probe immobilization protocol. Hence, the development of a simple and label-free electrochemical IgE aptasensor is highly demanded.

To circumvent the aforementioned problems, in the present contribution we brought in MWCNTs/IL nanocomposite and chitosan as immobilization interface together with aptamer probe as recognizing element and MB as electrochemical indicator. Chitosan (Chit) is a polysaccharide biopolymer which displays excellent film-forming ability, high water permeability, good adhesion, and susceptibility to chemical modifications due to the presence of reactive amino and hydroxyl functional groups (Zhang et al., 2004; Yi et al., 2005). The aptasensor is obtained by covalent immobilization of an amino-aptamer specific to IgE onto MWCNTs/IL/Chit nanocomposite modified GC electrode using glutaraldehyde (GA) as linking agent, followed by an equilibrated interaction with MB. In the presence of IgE, the interaction between aptamer and IgE displaces the MB from the electrode surface, rendering a lowered electrochemical signal attributed to decreased amount of adsorbed MB.

Although the basic concept of electrochemical biosensors based on aptamers and MB is not new, to the best of our knowledge, this concept has not applied for IgE detection thus far. In addition, the MWCNTs/IL/Chit nanocomposite used here can be considered as a novel substrate in designing aptasensors acting both as a platform to successful covalent immobilization of DNA aptamer with substantial loading ability and a promising tranducer with high surface to volume ratio and good electrical conductivity with the result of greatly improving sensor performance. The proposed aptasensor might seems complicated at first glance, but in comparison to most reported aptasensors, we believe that it could be considered as a simple system. It does not need any prelabeling step. In addition, the MWCNTs/IL/Chit nanocomposite is prepared through a simple and rapid one-step mixing procedure without need to any complicated and costly synthetic strategies. MB which acts as an electrochemical marker can be easily intercalated into the aptamer and the electrochemical signal arises from its reduction is very stable. The difficult aptamer based assays such as sandwich formats are avoided. Using this simple approach, it is possible to detect IgE low to picomolar concentrations.

## 2. Experimental

### 2.1. Chemicals and reagents

DNA aptamer (D17.4ext) with 5′-amino modification was custom-synthesized by Bioneer Co. (South Korea) and its base sequence is as follows (Maehashi et al., 2007):

D17.4ext: 5′-$NH_2$-GCG CGG GGC ACG TTT ATC CGT
CCC TCC TAG TGG CGT GCC CCG CGC-3′

IgE purified from human myeloma (Abcam, US) was diluted from a 20 g $l^{-1}$ stock solution in PBS (0.05 M, pH 7.4) and stored at −20 °C until use. Bovine serum albumin (BSA) and Lysozime were obtained from Sigma and dissolved in PBS (0.05 M, pH 7.4). MWCNTs with purity of 95%, surface specific area of 480 $m^2$ $g^{-1}$, diameter of 20–30 nm and 1 μm length were obtained from Nanolab (Brighton, MA). N-Butyl-N-methyl pyrolydinium bis (trifluoromethylsulfonyl) imide [$C_4$mpyr][$NTf_2$] (IL) was purchased from Sigma. Human serum sample for real sample analysis was supplied by a clinical diagnostic laboratory. MB, GA, $K_3Fe(CN)_6$ and $K_4Fe(CN)_6$ and all other reagents (from Merck or Fluka) were used as supplied (analytical or HPLC grade) without further purification. Phosphate buffer solutions (PBS) were prepared with $NaH_2PO_4$ and $Na_2HPO_4$ and used as supporting electrolyte throughout electrochemical studies. pH adjustment was performed with NaOH or HCl.

### 2.2. Apparatus

Surface morphology was examined using Vega-Tescan electron microscope. Cyclic voltammetry (CV), differential pulse voltammetry (DPV) and electrochemical impedance measurements (EIS) were performed on an AUTOLAB modular electrochemical system (ECO Chemie, Ultrecht, The Netherlands) equipped with a PGSTAT 101 module and driven by GPES and FRA softwares (ECO Chemie) in conjunction with a conventional three-electrode system and a personal computer for data storage and processing. A modified GC electrode employed as the working electrode and a platinum wire as the counter electrode. All potentials were referred to an Ag/AgCl/KCl (3 M) electrode. The impedance analysis was performed in the frequency range from 0.1 Hz to 100 kHz, using a

modulation voltage of 5 mV in 0.1 M KCl solution containing 5 mM $K_3[Fe(CN)_6]/K_4[Fe(CN)_6]$ (1:1) mixture as redox probe in. The Zview modeling program (version 2.3f) was used to fit the faradaic impedance spectra. Prior to performing experiments, the electrolyte solution was purged with $N_2$ for at least 10 min to remove dissolved $O_2$ and kept under $N_2$ atmosphere during measurements. All electrochemical measurements were performed at room temperature.

### 2.3. Preparation of the MWCNTs/IL/Chit/GC electrode

Prior to coating, GC electrode was subsequently polished with 3 and 0.95 μm alumina powders on polishing cloth and sonicated successively in ethanol and water in order to remove adsorbed particles. The nanocomposite was prepared by direct mixing of 0.25 mg chitosan, 3 mg MWCNTs and 10 μL IL, followed by grounding in an agate mortar until a homogeneous paste obtained. The MWCNTs/IL/Chit modified GC electrode was fabricated by rubbing some of this paste on the electrode surface to form a homogeneous layer. The effective surface area (A) for GC and MWCNTs/IL/Chit/GC electrodes was determined from cyclic voltammograms of 5 mM $K_3[Fe(CN)_6]$ in 0.1 M KCl solution. According to Eq. (1) (Bard and Faulkner 2001):

$$i_p = \left(2.69 \times 10^5\right) n^{3/2} A C D^{1/2} v^{1/2} \quad (1)$$

where $i_p$ is the peak current, $n$ is the number of electrons in the reaction, $A$ is the electrode area, $D$ is the diffusion coefficient of the oxidized form, hexacyanoferrate (III), $C$ is the bulk concentration of the oxidized form and $v$ is the scan rate. From the slope of the $i_p$ *vs.* $v^{1/2}$ line, the values of $A$ were determined as 0.0314 $cm^2$ and 0.15 $cm^2$ for GC and MWCNTs/IL/Chit/GC, respectively. Therefore, after GC electrode was modified with MWCNTs/IL/Chit nanocomposite film, the electroactive surface area greatly increased, indicating that the introduction of the nanocomposite provides more conduction pathways for the electron-transfer of $Fe(CN)_6^{3-/4-}$.

### 2.4. Fabrication of the sensing interface

The MWCNTs/IL/Chit/GC electrode was immersed in a 2.5% GA in PBS for 1 h. After rinsing, the IgE-specific 5'-amino-modified aptamer solution in 0.05 M PBS (10 μl, 10 μM) was added and incubated on the electrode surface for 12 h at room temperature. Then, the aptamer modified electrode was rinsed thoroughly with PBS in order to remove any unbounded aptamers followed by placing a 10 μl aliquot of 0.1 M PBS (pH 7.4) containing 1% BSA for 30 min on the electrode surface to reduce non-specific binding. After that, the electrode was placed in a 20 μM MB stirring solution (0.1 M PBS, pH 7.4) for 10 min to accumulate MB. Afterwards, the fabricated electrode (hereafter denoted as MB/Apt/MWCNTs/IL/Chit/GC) was successively rinsed with water and PBS and finally, it was immersed into IgE solution with different concentrations for 40 min. The schematic representation of the fabrication of IgE apatasensor is shown in Scheme 1. The electrochemical signals were obtained in PBS by using DPV with amplitude of 25 mV and pulse width of 0.05 s.

## 3. Results and discussion

### 3.1. Principle of IgE detection using MB/Apt/MWCNTs/IL/Chit/GC electrode

Scheme 1 presents the detailed detection process of the electrochemical aptasensor for human IgE. The GC electrode surface is first modified by a homogeneous film of MWCNTs/IL/Chit nanocomposite. This leads to increase the effective surface area of electrode and provides an enhanced loading surface for the subsequent immobilization of aptamer. The 5′-amino-modified aptamer is covalently attached to the amine groups of chitosan via the aid of GA acting as linking agent. Taking advantage of the well-established intercalation properties of MB with DNA (Tuite and Norden, 1994; Erdem et al., 2000) as well as due to its low cost and good redox characteristics, it was used as electrochemical indicator in our proposed system. It was realized that intercalation of MB into DNA was mediated by the interaction with two guanine bases, suggesting that minimum two base pairs of G–C coupling in the stem structure of the beacon aptamer may lead to its intercalation (Friedman and Brown, 1978; Fusimoto et al., 1994; Tuite and Kelley, 1995; Bang et al., 2005). Here, the intercalation of MB into the aptamer could produce a well-defined DPV signal depicted as "a" in Scheme 1. When IgE as target is introduced, the aptamer selectively binds with it during which the MB releases from the electrode surface and thus, a decrease in peak current of MB is observed (depicted as "b" in Scheme 1).

### 3.2. Characterization and optimization of sensing interface

The morphology of the MWCNTs/IL/Chit nanocomposite was investigated by the SEM technique and the result was presented in Fig. S1 (see Supplementary Material). As can be observed, the prepared nanocomposite shows a unique structure and forms a relatively homogeneous film. It may be suggested that MWCNTs and Chit have been uniformly integrated with Chit.

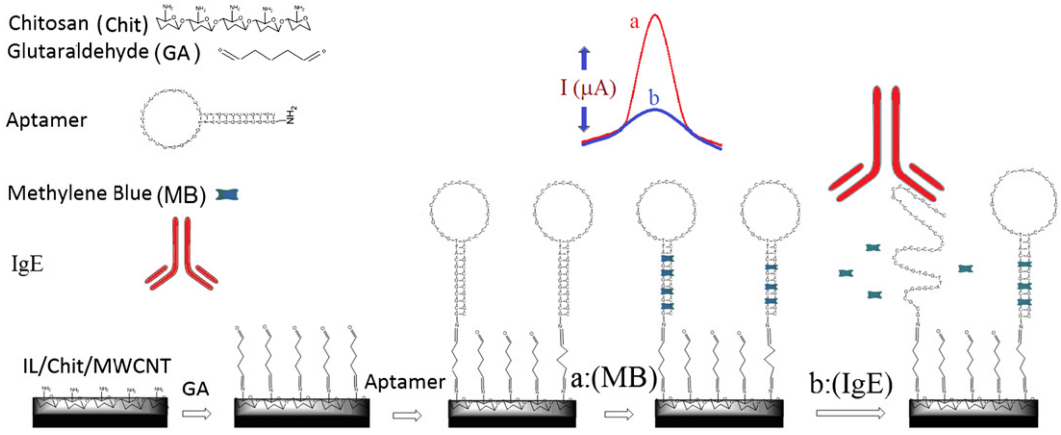


**Scheme 1.** Schematic outline of the principle for label-free electrochemical IgE biosensing.

In order to prove the superior performance of the MWCNTs/IL/Chit nanocomposite, CV of $[Fe(CN)_6]^{3-/4-}$ as a marker was studied at different electrodes of GC, MWCNTs/GC, MWCNTs/IL/GC and MWCNTs/IL/Chit/GC (Fig. S2). Well-defined redox characteristics of $[Fe(CN)_6]^{3-/4-}$ were observed for all of these electrodes but with variations in the current response and values of peak-to-peak separations ($\Delta E_p$). CV of $[Fe(CN)_6]^{3-/4-}$ redox probe at GC exhibits peaks with $\Delta E_p$ as $\sim$0.22 V. A marked increase in current as well as a decrease in $\Delta E_p$ ($\sim$0.09 V) was noticed at MWCNTs/GC electrode as compared to GC, which can be ascribed to the large electron transfer capability and high specific surface area of MWCNTs. MWCNTs/IL/GC exhibited an increased $\Delta E_p$ (0.14 V) as compared to MWCNTs/GC electrode. The anodic peak current of $[Fe(CN)_6]^{3-/4-}$ is higher at MWCNTs/IL/GC than at MWCNTs/GC electrode. Interestingly, when Chit was added to the MWCNTs/IL, although the $\Delta E_p$ value increased and reached to 0.16 V from 0.14 V (MWCNTs/IL/GC), the current response of the electrode increased substantially, indicating that the introduction of this nanocomposite provides more conduction pathways for electron transfer of $[Fe(CN)_6]^{3-/4-}$ compared to other electrodes. In fact, in spite of our expectation that existence of Chit may lead to decrease the electroactivity of electrode due to its insulating nature, however, in the present study, it was found through CV results that the IL/Chit layer could retain electron transfer path. The larger surface area and more facilitated dispersion of MWCNTs in the MWCNTs/IL/Chit nanocomposite may be the reasons for the observed behavior.

CV was further applied to follow the barrier changes of the electrode surface before and after each assembly step. To being able to better compare the changes in electroactivity of the electrode, CVs of $[Fe(CN)_6]^{3-/4-}$ at GC and MWCNTs/IL/Chit/GC have been shown. A couple of well-defined redox peaks could be observed at the bare GC which after the electrode modification with MWCNTs/IL/Chit nanocomposite, the current response increased obviously. The current response at the Apt/MWCNTs/IL/Chit/GC decreased dramatically as compared with that at the MWCNTs/IL/Chit/GC and $\Delta E_p$ became 0.18 V. This implies that most of the electrode surface is covered by aptamer, with the result of blocking the electron-transfer efficiency of $[Fe(CN)_6]^{4-/3-}$ at solid/liquid interface due to this fact that the electrostatic repulsion between anionic $[Fe(CN)_6]^{3-/4-}$ and the surface bound aptamer DNA sequences with negative charges retards the interfacial electron-transfer kinetics. This observation demonstrates that the covalent immobilization of aptamer has been achieved successfully. The incubation with 5 nM human IgE for 40 min gave rise to further decrease in peak current as well as an increase in $\Delta E_p$ to 0.26 V. It means that human IgE is adsorbed onto the electrode surface with the result of substantially hindering the electron transfer between the electrode surface and redox couples in solution due to the opening of the stem part of aptamer and the formation of IgE/aptamer complex.

In order to further confirm that the sensing interface is constructed successfully, we utilized EIS to monitor the impedance change of electrode after each of modification steps is applied. The impedance spectra include a semicircle portion at higher frequencies relating to the electron transfer-limited process and a linear part at lower frequencies corresponding to diffusion. The increase in the diameter of the semicircle reflects the increase in the interfacial electron transfer resistance. Fig. 1B displays the Nyquist plots obtained with the GC, MWCNTs/IL/Chit/GC and Apt/MWCNTs/IL/Chit/GC electrode before and after incubated with different concentrations of IgE (5, 10, 15, 20 and 25 nM) in 0.1 M KCl solution containing 5 mM $Fe(CN)_6^{3-/4-}$. The impedance spectra were fitted to a modified randle's equivalent circuit, as shown in the inset (A) of Fig. 1B, where $R_s$ represents the electrolyte resistance, $C_{dl}$ is the double-layer capacitance, $R_{ct}$ is the charge-transfer resistance and $Z_w$ is the Warburg impedance (Huang et al., 2002; Yan et al., 2008). The higher frequency range portion of the spectra was shown in the inset (B) of Fig. 1B. The line passing through the data points represents the fits using the equivalent circuit. Its superposition on the data points indicated a good match of the model with the measured data. Table 1A shows the values of the equivalent circuit elements obtained by the experimental data fitting as well as the correspondent relative standard deviations (RSD) in determining each of different elements. From the RSD values in Table 1A given in parentheses for each element, it can be concluded that the proposed system possess a satisfactory level of reproducibility during independent measurements. The change in the values of $R_{ct}$ for different modified electrodes was chosen to study the surface properties during fabrication process of aptamer-based biosensor. As shown, significant differences in the charge transfer resistance ($R_{ct}$) were observed upon the stepwise formation of the modified electrode. At first, it can be seen that for MWCNTs/IL/Chit/GC electrode, the value of $R_{ct}$ decreases compared to the bare GC electrode due to the higher electron transfer ability and electronic conductivity of the MWCNTs present in the nanocomposite. With the immobilization of aptamer probe onto the MWCNTs/IL/Chit nanocomposite modified electrode in the next step, $R_{ct}$ increases to 375.9 Ω that could be attributed to the repulsion between negative charges of aptamer phosphate groups and $Fe(CN)_6^{4-/3-}$ molecule. Incubation of the electrode with 5 nM IgE led to increasing the $R_{ct}$ value up to 568.2 Ω. With increasing the IgE concentrations (10, 15, 20 and 25 nM), the relevant increase in $R_{ct}$ value became larger and reached to 685.5, 873.2, 998.3 and 1446 Ω, respectively, suggesting that IgE/aptamer interaction well achieved at the electrode surface. As shown in the inset (C) of the Fig. 1B which shows evolution of $R_{ct}$ as a function of IgE concentration, the $R_{ct}$ value linearly increased with increasing IgE concentration. This clearly indicates that the proposed aptasensor can also be used as an efficient impedimetric biosensor for IgE detection. The herein obtained impedance data corroborate the preceding results obtained by CV, all demonstrate that the sensing interface is constructed successfully.

To investigate the kinetic parameters of the modified electrode, CVs of MB/Apt/MWCNTs/IL/Chit/GC electrode at different scan rates were recorded and the results were shown in Fig. 2. As illustrated, a well-defined redox couple with $E^{\circ\prime} = -0.2$ V (*vs.* Ag/AgCl) was observed corresponding to intercalated MB. The peak currents of the redox system were directly proportional to the scan rate for sweep rates below 1.0 V $s^{-1}$ (inset A of Fig. 2) as expected for a redox surface controlled process. The peak-to-peak potential separation was about 80 mV for sweep rates below 100 mV $s^{-1}$, reflecting facile charge transfer kinetics over this range of sweep rate. At higher sweep rates ($\nu > 1000$ mV$s^{-1}$), peak separations began to increase (inset B of Fig. 2), indicating limitation due to the charge transfer kinetics. Based on the Laviron theory (Laviron, 1979), the heterogeneous electron transfer rate constant ($k_s$) and charge transfer coefficient ($\alpha$) can be determined by measuring the variation of peak potential with scan rate. The values of peak potentials were proportional to $\log(\nu)$ for scan rates higher than 2.0 V $s^{-1}$. Using the equation $E_p = K - 2.303\ (RT/\alpha nF)\ \log \nu$, where $K = E^{\circ\prime} - 2.303\ (RT/\alpha nF) \log(RTk_s/nF)$, charge transfer coefficient ($\alpha$) for proposed redox couple was calculated. Through introducing this value in the following Eq. (2), an apparent surface electron transfer rate constant ($k_s$) was estimated:

$$\log k_s = \alpha\log(1-\alpha) + (1-\alpha)\log\alpha - \log(RT/\mathrm{nF}\nu) - \alpha(1-\alpha)nF\Delta E/2.303RT \quad (2)$$

The values of $k_s$ and $\alpha$ were obtained as 6.3 $s^{-1}$ and 0.56, respectively. The value of $k_s$ implies high ability of MWCNTs/IL/Chit

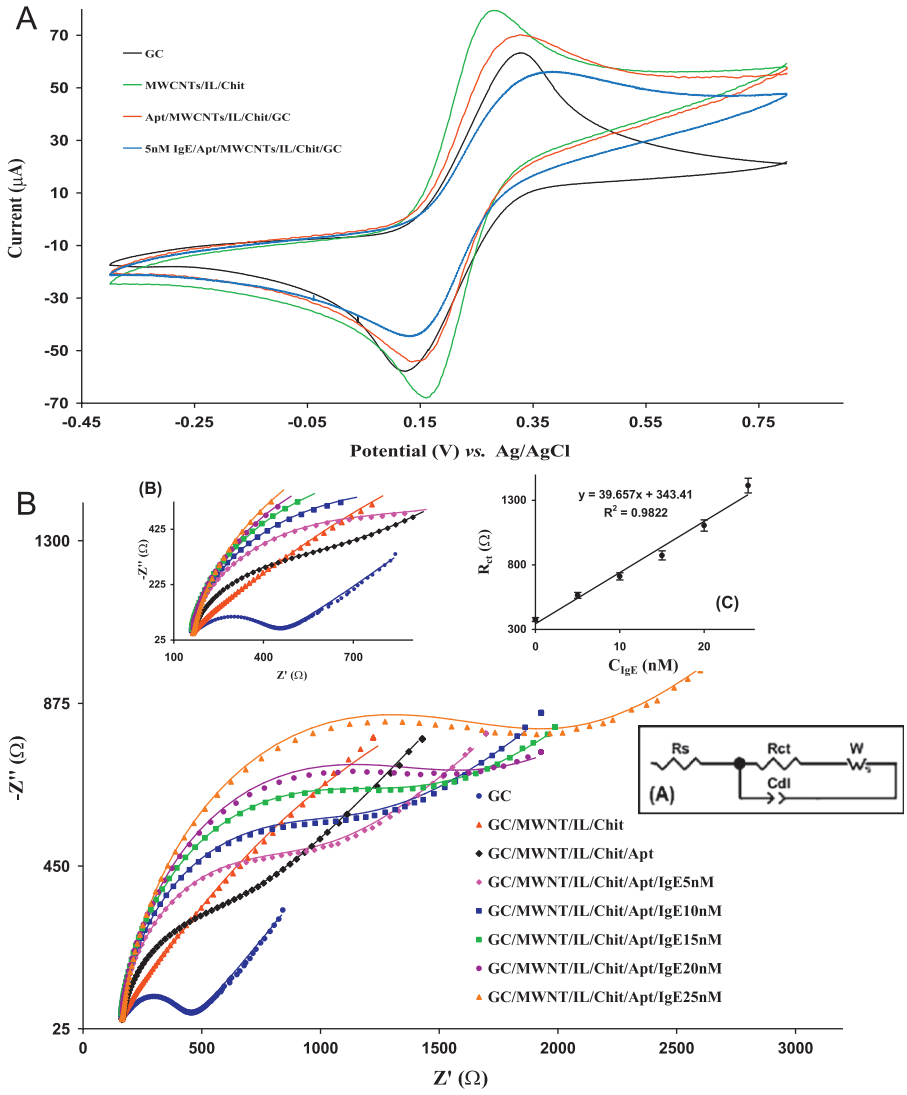


**Fig. 1.** (A) CVs and (B) Nyquist curves of 5.0 mM $[Fe(CN)_6]^{3-/4-}$ in 0.1 M KCl recorded at bare GC, MWCNTs/IL/Chit/GC, Apt/MWCNTs/IL/Chit/GC and Apt/MWCNTs/IL/Chit/GC after incubated with 5, 10, 15, 20 and 25 nM IgE (scan rate in A is 0.1 V $s^{-1}$; frequency range in B is 0.1–10 kHz). Insets of Fig. 1B are as follows: (A) the equivalent circuit used to fit the experimental impedance data; (B) higher frequency range portion of the Nyquist curves for different electrodes; and (C) the corresponding calibration plot for variation of $R_{ct}$ *vs.* IgE concentration.

**Table 1A**
Values of equivalent circuit elements ($R_s$, $C_{dl}$ and $R_{ct}$) obtained for fitting of the experimental data for different electrodes; the figures in parentheses refer to the RSD for each value ($n=3$).

| | $R_s$ (Ω) | $C_{dl}$ (μF) | $R_{ct}$ (Ω) |
|---|---|---|---|
| GC | 660.4(3.36) | 1.867(3.43) | **282.2(1.83)** |
| GC/MWNT/IL/Chit | 127.0(5.94) | 149.240(6.26) | – |
| GC/MWNT/IL/Chit/Apt | 167.0(5.41) | 4.460(4.28) | **375.9(4.87)** |
| GC/MWNT/IL/Chit/Apt/ IgE (5 nM) | 157.1(5.20) | 2.234(5.09) | **568.2(4.28)** |
| GC/MWNT/IL/Chit/Apt/IgE(10 nM) | 182.6(5.89) | 2.156(4.14) | **685.5(4.85)** |
| GC/MWNT/IL/Chit/Apt/IgE(15 nM) | 161.0(4.60) | 2.358(3.61) | **873.2(4.92)** |
| GC/MWNT/IL/Chit/Apt/IgE(20 nM) | 159.2(5.07) | 2.056(4.15) | **998.3(2.74)** |
| GC/MWNT/IL/Chit/Apt/IgE(25 nM) | 158.3(4.76) | 2.363(5.87) | **1446.0(2.02)** |

nanocomposite for promoting electron transfer between redox couple and electrode surface. The large number of structural defects on the MWCNTs surface as well as its special nanostructure may act as molecular wires, enhance the direct electron transfer redox systems at MWCNTs/IL/Chit nanocomposite interface.

In addition, stability investigation of the redox system resulted from MB revealed that its voltammetric behavior is very stable and only 3% reduction in peak current was observed after 100 repetitive cycles (Fig. S3). Additionally, the storage stability of the modified electrode was very good as the electrode was found to have reserved (95%) its initial activity for more than 2 weeks

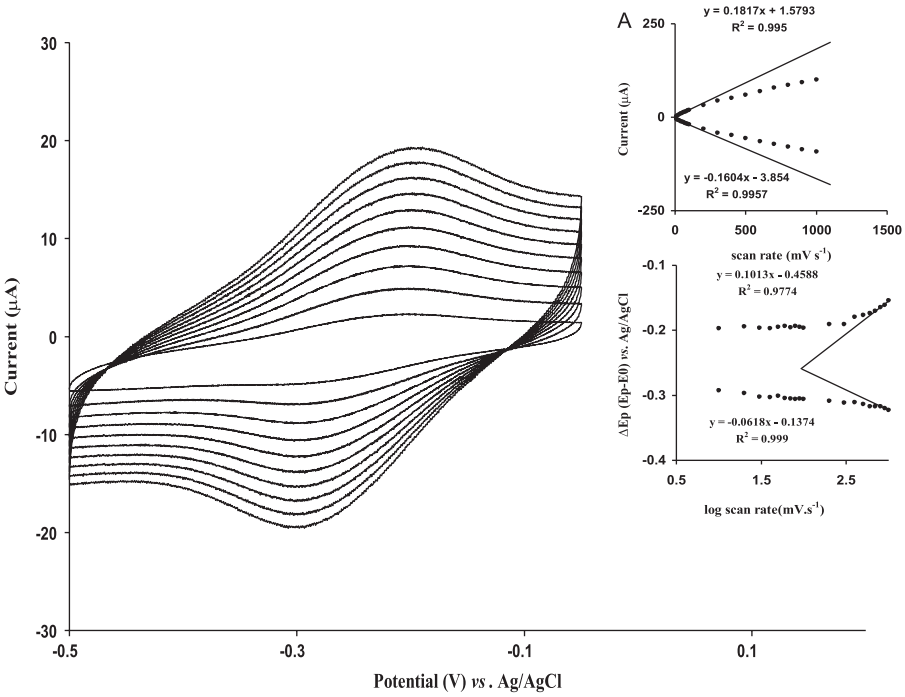


**Fig. 2.** CV responses of MB/Apt/MWCNTs/IL/Chit/GC electrode in PBS (0.1 M, pH 7.4) at scan rates (from inner to outer) 10, 20, 30, 40, 50, 60, 70, 80, 90, and 100 m V $s^{-1}$. Inset A is the plot of peak current *vs.* scan rate and Inset B is the variation of peak potential separation *vs.* log of scan rate.

when kept at 4 °C. This high stability may be ascribed to the chemical and mechanical stability of MWCNTs/IL/Chit nanocomposite as well as its compatibility with the aptamer covalently attached on its surface which indicates the promising properties of MWCNTs/IL/Chit as a useful platform for immobilization of aptamer sequences.

The sensor response is a strong function of probe density. The effect of aptamer concentration on the current signal of the sensor was explored and the results were presented in Fig. S4. From this figure, it is indicative that the sensor sensitivity is clearly dependent on the aptamer concentration: as the concentration of aptamer probe increases, the sensor signal increases to a maximum and then decreases substantially. The poorer signaling of the sensor at higher concentrations of aptamer may be due to the inactivation of some aptamers, reducing the response as fewer of the probes undergo binding with target proteins. This inactivation could result from steric/conformational restrictions and unfavorable interactions between neighboring aptamers such as cross hybridization that is a potential result of the self-complimentary nature of the individual aptamer sequences. Therefore, 10 μM was selected as optimized aptamer concentration and used in throughout experiments.

The incubation time for the interaction of IgE and the surface-bound aptamer probe was studied as another factor affecting the analytical performance of the present biosensor (Fig. S5). The obtained results indicate that the current response increases rapidly with the increment of incubation time up to 40 min and then reaches a plateau, indicating the interaction reached to steady state. Therefore, 40 min incubation time was chosen for binding of IgE protein to the aptamer modified electrode in throughout experiments.

### 3.3. Analytical characteristics of the IgE aptasensor

To ensure the present assay platform can be used for sensitive quantification of target protein, the current responses induced by IgE at different concentrations are evaluated. Fig. 3 shows the

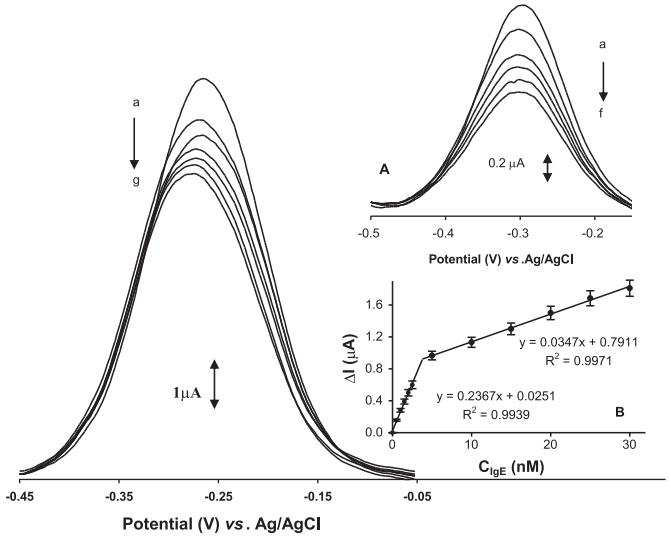


**Fig. 3.** DPVs of MB/Apt/MWCNTs/IL/Chit/GC electrode after incubation for 40 min with different IgE concentrations of (from outer to inner) 0, 5, 10, 15, 20, 25 and 30 nM in PBS (0.1 M, pH 7.4). Inset A shows DPVs of MB/Apt/MWCNTs/IL/Chit/GC electrode for lower concentrations of IgE: (from outer to inner) 0.0, 0.5, 1.0, 1.5, 2.0 and 2.5 nM. Inset B is the plot of current response *vs.* IgE concentration (the measurements were carried out in triplicate).

electrochemical response to different concentrations of IgE. As is obvious from the figure, the peak current signals decrease with the increase of IgE concentration. Through analyzing the change between current of MB reduction peak and the concentrations of IgE, a linear relation between the current response and the IgE concentration was observed in two concentration ranges. For lower concentration range that is from 0.5 to 2.5 nM (inset A of Fig. 3), the following equation between current response and the IgE concentration was found; $\Delta I(\mu A) = 0.0347\ C(nM) + 0.7911\ \mu A$, $R^2 = 0.9971$, whereas for higher concentration range (5–30 nM), the corresponding equation is as follows: $\Delta I(\mu A) = 0.2367C(nM) + 0.0251\ \mu A$,

$R^2$=0.9939 (inset B of Fig. 3). The detection limit was calculated as 37 pM (based on $S/N=3$). The reason for observing two linear concentration ranges with different slopes is that the amount of aptamer immobilized on the electrode surface is some certain. When the sensor is used to detecting IgE at low concentrations, IgE can readily interact with the abundant active sites of aptamer present on the electrode surface. With increasing IgE concentration, the active sites of aptamer available on the electrode surface for interacting with IgE target molecules become fewer. Therefore, the sensitivity declines when the aptasensor is used to determine higher concentractions of IgE and calibration curves with different slopes are observed. This phenomenon was also reported for some other aptasensors (Yang et al., 2009; Ding et al., 2010; Wang et al., 2009c).

Table 1B lists the response characteristics of the proposed IgE aptasensor compared to the some other electrochemical or optical aptasensors reported in the literature. The results presented in Table 1B obviously show that the different characteristics of the proposed strategy for IgE biosensing are better in some cases or comparable with the other sensors reported so far.

The reproducibility of the aptasensor is a very important feature, and thus the parameter was estimated. Six repetitive measurements of 5 nM of IgE solution with the proposed biosensor was used for estimating the precision of the aptasensor. The results indicated acceptable and reproducible signals with RSD of 4% were obtained. Furthermore, in order to study the reproducibility of the aptasensor fabrication strategy, five MB/Apt/MWCNTs/IL/Chit/GC electrode prepared independently. The RSD of the aptasensors responses toward 5 nM of IgE was 5%, which indicated that the detection results based on the proposed strategy are reproducible and the aptasensor is of good reproducibility.

### 3.4. The selectivity of biosensor for IgE detection

An excellent electrochemical aptasensor has to illustrate good selectivity. In order to investigate the binding specificity of the aptasensor toward IgE, control experiments were performed under the same experimental conditions. For this purpose, two compounds of BSA and Lysozyme were chosen as the interfering proteins. Since Lysozyme has a very high basic charge (p$I$=9.1) and is known to bind nonspecifically to nucleic acids, hence, it can be a good control experiment. The concentration of the BSA was chosen to be very high, as in the case of serum samples. Fig. 4 exhibits different current response signals of the proposed sensing system after the addition of 40 nM Lysozyme (Fig. 4A), 1% BSA (Fig. 4B) and 3 nM IgE (Fig. 4C). As can be seen, while the decrease of MB reduction peak current is very small after the electrode reacted with BSA and Lysozyme, a significant decrease induced by the interaction of the aptamer probe and IgE was observed. This can be ascribed to this fact that the binding event between IgE and aptamer is based on the specific recognition between them but not on the other factors, such as nonspecific protein adsorption. Therefore, the proposed strategy has a sufficient specificity to IgE against other proteins and IgE could be identified with high selectivity.

**Table 1B**
Response characteristics of different aptamer-based IgE biosensors.

| Analytical method | DLR (nM) | LOD (pM) | Ref. |
|---|---|---|---|
| Fluorescence anisotropy | 1–60 | 350 | Gokulrangan et al. (2005) |
| Luminescence | – | 100 | Jiang et al. (2004) |
| FET | 0.25–20 | 250 | Maehashi et al. (2007) |
| AC voltammetry | 0.36–54 | 36 | Wu et al. (2009) |
| EIS | 2.5–100 | 100 | Xu et al. (2005) |
| EIS | 0.5–5 | | Wang et al. (2009b) |
| DPV | 0.5–30 | 37 | This work |

### 3.5. The IgE determination in serum samples

In order to estimate the applicability of the methodology, the proposed IgE aptasensor was tested by applying it to the analysis of IgE concentration in a human serum sample by the DPV technique. The standard addition method was adopted for this purpose and the obtained result was compared with the determined value through a standard ELISA method. Performed measurements gave 0.96 ($\pm$0.03) nM (the average of three replicate measurements) for IgE concentration in serum sample which is very close to that obtained by standard ELISA method (0.90 nM) ( Fig. S6). It could be seen that there is a good agreement between results obtained by two methods and thus, the MB/Apt/MWCNTs/IL/Chit/GC electrode might be a promising system for detecting IgE in real samples.

## 4. Conclusion

In summary, a simple and label-free electrochemical aptasensor was developed utilizing MWCNTs/IL/Chit nanocomposite as a promising transduction platform on the electrode surface and MB as an effective redox indicator. Due to the unique properties of vast surface-to-bulk ratio and good electrical conductivity as well as abundant reactive amine groups, MWCNTs/IL/Chit nanocomposite function as a signal amplifier to facilitate both the immobilization of the aptamer probe on its surface and the electron-transfer between the MB and the electrode. The human

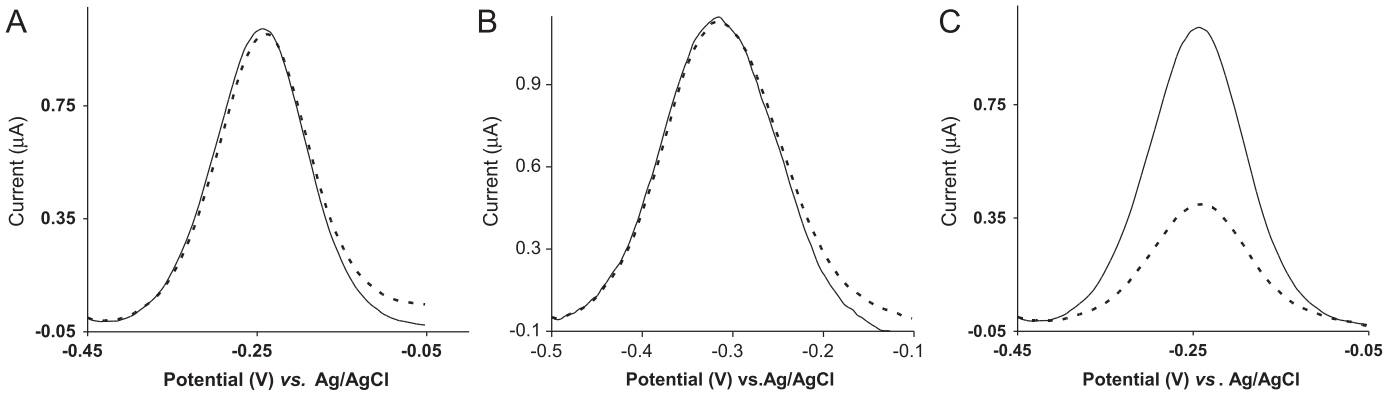


**Fig. 4.** The DPVs of MB/Apt/MWCNTs/IL/Chit/GC electrode before (solid line) and after (dashed line) being incubated for 40 min with (A) 40 nM Lysozyme, (B) 1% BSA and (C) 3 nM IgE. Electrolyte: PBS (0.1 M, pH 7.4).

IgE was used as the model target protein to demonstrate the feasibility of the proposed methodology as a proof of concept. Here, the cathodic peak current of MB linearly decreases by the addition of IgE in concentration range of 0.5 to 30.0 nM. The estimated detection limit of the IgE was 37 nM. This method can specifically recognize IgE, other proteins such as BSA and Lysozyme did not affect the detection and it has been applied in real sample with satisfactory result. For all, the proposed aptasensor has been demonstrated to offer a convenient, specific, and sensitive method not only for detecting IgE as a model system but it also possess the potential to be applied for other targets detection.

## Acknowledgments

This research was supported by the Iranian Nanotechnology Initiative and the Research Office of the University of Kurdistan We thanks Mrs Ensiyeh Sharifi (Isfahan University) for her corporations in fitting of impedance data. The authors also thank Dr. Asaad Vaziri and Dr. Verdi's Clinical Laboratory for IgE detection in serum sample by ELISA technique.

## Appendix A. Supporting information

Supplementary data associated with this article can be found in the online version at http://dx.doi.org/10.1016/j.bios.2012.12.006.

## References

Bang, G.S., Cho, S., Kim, B.G., 2005. Biosensors and Bioelectronics 21, 863–870.
Bard, A.J., Faulkner, L.R., 2001. Electrochemical Methods, Fundamentals and Applications, 2nd ed. John Wiley and Sons, New York.
Baughman, R.H., Zakhidov, A.A., de Heer, W.A., 2002. Science 297, 787–792.
Chen, R.J., Zhang, Y., Wang, D., Dai, H., 2001. Journal of the American Chemical Society 123, 3838–3839.
Cheng, A.K.H., Ge, B., Yu, H.Z., 2007. Analytical Chemistry 79, 5158–5164.
Ding, C., Ge, Y., Lin, J.M., 2010. Biosensors and Bioelectronics 25, 1290–1294.
Du, Y., Li, B., Wang, F., Dong, S., 2009. Biosensors and Bioelectronics 24, 1979–1983.
Ellington, A.D., Szostak, J.W., 1990. Nature 346, 818–822.
Erdem, A., Kerman, K., Meric, B., Akarca, U.S., Ozsoz, M., 2000. Analytica Chimica Acta 422, 139–149.
Feng, K., Sun, C., Kang, Y., Chen, J., Jiang, J.H., Shen, G.L., Yu, R.Q., 2008. Electrochemistry Communications 10, 531–535.
Friedman, T., Brown, D.M., 1978. Nucleic Acids Research 5, 615–622.
Fukushima, T., Kosaka, A., Ishimura, Y., Yamamoto, T., Takigawa, T., Ishii, N., Aida, T., 2003. Science 300, 2072–2074.
Fusimoto, B.S., Clendenning, J.B., Delrow, J.J., Heath, P.J., Schurr, M., 1994. Journal of Physical Chemistry 98, 6633–6643.
Gokulrangan, G., Unruh, J.R., Holub, D.F., Ingram, B., Johnson, C.K., Wilson, G.S., 2005. Analytical Chemistry 77, 1963–1970.
Gooding, J.J., Wibowo, R., Liu, J.Q., Yang, W.R., Losic, D., Orbong, S., Mearns, F.J., 2003. Journal of the American Chemical Society 125, 9006–9007.
Ho, H.A., Leclerc, M., 2004. Journal of the American Chemical Society 126, 1384–1387.
Huang, W., Zhang, Z., Han, X., Wang, J., Tang, J., Dong, S., Wang, E., 2002. Biophysical Chemistry 99, 271–279.
Jiang, Y., Fang, X., Bai, C., 2004. Analytical Chemistry 76, 5230–5235.
Kang, Y., Feng, K.J., Chen, J.W., Jiang, J.H., Shen, G.L., Yu, R.Q., 2008. Bioelectrochemistry 73, 76–81.
Kara, P., Kerman, K., Ozkan, D., Meric, B., Erdem, A., Ozkan, Z., Ozsoz, M., 2002. Electrochemistry Communications 4, 705–709.
Kerman, K., Ozkan, D., Kara, P., Meric, B., Gooding, J.J., Ozsoz, M., 2002. Analytica Chimica Acta 462, 39–47.
Kim, Y.H., Kim, J.P., Han, S.J., Sim, S.J., 2009. Sensors and Actuators B: Chemical 139, 471–475.
Laviron, E., 1979. Journal of Electroanalytical Chemistry 101, 19–28.
Li, D., Muller, M.B., Gilje, S., Kaner, R.B., Wallace, G.G., 2008. Nature Nanotechnology 3, 101–105.
Liu, A., Chen, X., Wang, K., Wei, N., Sun, Z., Lin, X., Chen, Y., Du, M., 2011. Sensors and Actuators B: Chemical 160, 1458–1463.
Maehashi, K., Katsura, T., Kerman, K., Takamura, Y., Matsumoto, K., Tamiya, E., 2007. Analytical Chemistry 79, 782–787.
Nutiu, R., Li, Y., 2003. Journal of the American Chemical Society 125, 4771–4778.
Papamichael, K.I., Kreuzer, M.P., Guilbault, G.G., 2007. Sensors and Actuators B: Chemical 121, 178–186.
Pavlov, V., Xiao, Y., Shlyahovsky, B., Willner, I., 2004. Journal of the American Chemical Society 126, 11768–11769.
Radi, A.E., Sánchez, J.L.A., Baldrich, E., O'Sullivan, C.K, 2005. Analytical Chemistry 77, 6320–6323.
Rao, C.N.R., Satishkumar, B.C., Govindaraj, A., Nath, M., 2001. ChemPhysChem 2, 78–105.
Salimi, A., Noorbakhsh, A., Soltanian, S., 2006. Electroanalysis 18, 703–711.
Salimi, A., Mamkhezri, H., Hallaj, R., Zandi, S., 2007. Electrochimica Acta 52, 6097–6105.
Salimi, A., Lashgari, S., Noorbakhsh, A., 2010. Electroanalysis 22, 1707–1716.
Sutton, B.J., Gould, H.J., 1993. Nature 366, 421–428.
Teymourian, H., Salimi, A., Hallaj, R., 2012a. Talanta 90, 91–98.
Teymourian, H., Salimi, A., Hallaj, R., 2012b. Biosensors and Bioelectronics 33, 60–68.
Tuerk, C., Gold, L., 1990. Science 249, 505–510.
Tuite, E., Norden, B., 1994. Journal of the American Chemical Society 116, 7548–7556.
Tuite, E., Kelley, J.M., 1995. Biopolymers 35, 419–433.
Wang, J., Lv, R., Xu, J., Xu, D., Chen, H., 2008. Analytical and Bioanalytical Chemistry 390, 1059–1065.
Wang, J., Wang, F., Dong, S., 2009a. Journal of Electroanalytical Chemistry 626, 1–5.
Wang, J., Xu, D., Chen, H.Y., 2009b. Electrochemistry Communications 11, 1627–1630.
Wang, J., Meng, W., Zheng, X., Liu, S., Li, G., 2009c. Biosensors and Bioelectronics 24, 1598–1602.
Wang, Q., Tang, H., Xie, Q., Tan, L., Zhang, Y., Li, B., Yao, S., 2007. Electrochimica Acta 52, 6630–6637.
Wu, Z.S., Zheng, F., Shen, G.L., Yu, R.Q., 2009. Biomaterials 30, 2950–2955.
Xu, D., Xu, D., Yu, X., Liu, Z., He, W., Ma, Z., 2005. Analytical Chemistry 77, 5107–5113.
Yan, F., Wang, F., Chen, Z., 2011. Sensors and Actuators B: Chemical 160, 1380–1385.
Yan, J., Song, H., Yang, S., Yan, J., Chen, X., 2008. Electrochimica Acta 53, 6351–6355.
Yang, H., Ji, J., Liu, Y., Kong, J., Liu, B., 2009. Electrochemistry Communications 11, 38–40.
Yao, C., Qi, Y., Zhao, Y., Xiang, Y., Chen, Q., Fu, W., 2009. Biosensors and Bioelectronics 24, 2499–2503.
Yi, H., Wu, L.Q., Bentley, W.E., Ghodssi, R., Rubloff, G.W., Culver, J.N., Payne, G.F., 2005. Biomacromolecules 6, 2881–2894.
Zayats, M., Huang, Y., Gill, R., Ma, C., Willner, I., 2006. Journal of the American Chemical Society 128, 13666–13667.
Zhang, M., Smith, A., Gorski, W., 2004. Analytical Chemistry 76, 5045–5050.